1988

Heat Transfer and Component Temperature Prediction in Reciprocating Compressors

Rifat Keribar
Integral Technologies Incorporated

Thomas Morel
Integral Technologies Incorporated

HEAT TRANSFER AND COMPONENT TEMPERATURE PREDICTION IN RECIPROCATING COMPRESSORS

Rifat Keribar and Thomas Morel

Integral Technologies Incorporated
Westmont, Illinois 60559

ABSTRACT

A number of compressor design and performance issues are influenced by the heat transfer process. Specifically, the compressor power, outlet temperature and amount of heat rejected to the cooling system all depend on the overall level of heat transfer inside the cylinder/piston assembly. The spatial distribution of the in-cylinder heat flux has an effect on component thermal loading and the resulting component temperatures, thermal stresses and distortions. Advanced compressor designs which approach and exceed current design limits require accurate assessment and prediction of heat transfer. New methodology has been developed, which includes gas-to-wall heat transfer calculations based on in-cylinder flow velocities and they can be used to predict heat transfer in compressors as a function of speed, pressure ratio, fluid properties and compressor valve and piston geometry. These are coupled with a finite element based calculation of heat conduction in the structure to provide simultaneous solution for component temperatures, providing a complete performance and thermal characterization of the compressor.

INTRODUCTION

Heat transfer is one of the important processes which influence compressor design. One aspect of heat transfer concerns the loss of energy from the in-cylinder gases, which reduces the amount of piston work, and a parallel consideration relates to durability of compressor components exposed to often high temperatures. In an optimum compressor design, the amount of cooling applied should be carefully considered. Optimization of compressor cooling requires the solution of the coupled problem of heat transfer between gases and walls and of heat conduction through the structure. The heat conduction portion of such a calculation can be carried out to acceptable accuracy, using finite element models (FEM). By contrast, gas-to-wall heat transfer modeling is still in a developmental state. This presents a major stumbling block, since the gas-to-wall heat transfer correlations are needed to provide the necessary boundary conditions for the FEM codes. The calculated temperature field in the structure depends very critically on these boundary conditions, which must be well grounded in physics, if they are to provide an accurate description of the heat flux rates.

The model for in-cylinder convective heat transfer described below advances the state-of-the-art in that it gives a more accurate and more detailed description of the heat flux distribution in the cylinder. When used in a thermodynamic cycle model, it gives a more accurate description of the effects of heat transfer on compressor performance. Its use in conjunction with FEM codes improves the ability to address the issues related to maximum material temperatures, temperatures of lubricated surfaces in sliding contact, and of cooling load carried by coolant and by lubricating oil. The heat transfer models described here have been implemented and are being used in a comprehensive compressor simulation code IRIS-C, described in greater detail in a separate paper at this conference (1).

PREVIOUS CONVECTIVE HEAT TRANSFER MODELS

The standard approach to modeling of convective heat transfer is to assume that the heat flux may be described by an expression

$$q(t) = h_g(t)\,[T_g(t) - T_w(A)] \qquad (1)$$

where h_g is heat transfer coefficient, T_g is the gas temperature outside the thermal boundary layer, T_w is the wall temperature and A is the local surface area. Most of this work has been done in the engine context. The main differences between the various approaches stem from the definitions of h_g employed. Surveying the history of these approaches one finds that they can be divided into three "generations", starting with simple dimensional models, to more fundamentally based dimensionless

models, and, finally, to models that attempt to describe in some detail the fluid motions that drive the convective heat transfer.

Early Dimensional Models

These were the first models which date back over 60 years. The first, apparently, was the model of Nusselt (2). This model was used for many years, although it was based on data from a quiescent bomb not representative of actual engines. Another difficulty was that the model was not dimensionless and that presented scaling problems. Another early, widely used model was that due to Eichelberg (3). As with the Nusselt's model, the main drawback was again the lack of physics and the difficulty in scaling due to the dimensional form of the expression.

Second "Generation" Dimensionless Models

Based on reexamination of all data available, Annand (4) proposed that the proper dimensionless form is

$$Nu = a\,Re^{b} \tag{2}$$

where the pertinent length scale is taken to be the bore and the velocity scale as mean piston speed. This expression follows the lines of the well-known Reynolds analogy between heat and momentum transfer in fully developed turbulent boundary layers. The value of the exponent b was chosen to be 0.7, and the corresponding value of a was found to be between 0.35 and 0.80 depending on the "intensity of the charge motion". The widely used Woschni (5) correlation follows this general approach, with the exponent b = 0.8.

Third "Generation" Flow-Based Models

The previous classes of models represented the effects of fluid motions only tangentially through the use of V_p. However, the actual crank angle by crank angle variation of gas velocities is not represented, nor are the changes from compressor to compressor. These are serious shortcomings, which make the models insensitive to design details that are well known to significantly affect heat transfer, such as valve size and shape, and in-cylinder geometry. The role of turbulence in heat transfer was first explicitly considered by Borgnakke, et al (6) and Davis and Borgnakke, (7), who proposed the solution of a global two equation k and ϵ turbulence model for the cylinder. Important omissions of their model, however, are the neglect of the mean flow effects on heat transfer and lack of spatial resolution.

PRESENT CONVECTIVE HEAT TRANSFER MODEL

The present heat transfer model attempts to account for all of the important in-cylinder motions, and introduces the needed differentiation between the cylinder surfaces. The model is global in nature in that the Navier-Stokes equations are not solved in a formal sense, but it incorporates a low-resolution flow grid and much more physics than previous models, and thus it is expected to require much less adjustment from compressor to compressor than previous models. In fact, the model has no adjustable constants. It has been used on a wide range of engines and its predictions have been found consistently to be in good agreement with the heat rejection levels observed in test cell experiments.

The model is based on well established boundary layer concepts, as described in detail in Morel and Keribar (8), where specific application to diesel engines was discussed. The present work relates to a straightforward extension of the model to compressors. The starting point for the model is the instantaneous heat flux equation written in terms of the heat transfer coefficient h_g

$$q(t,A) = h_g(t,A)\,[T_g(t,A) - T_w(t,A)] \tag{4}$$

The convective heat transfer is assumed to be driven by fluid motions and the coefficient of the convective heat transfer is assumed to be related to the strength of the fluid motions through the Colburn analogy

$$h_g = 1/2\; C_f\; \rho\; U_{eff}\; C_p\; P^{-2/3} \tag{5}$$

where U_{eff} is an effective velocity outside a boundary layer at a particular surface location, ρ is average boundary layer density, C_f is a skin friction coefficient, C_p is the heat capacity of the gas and P is the Prandtl number. Inspection of equation (5) shows that the heat transfer coefficient is mainly driven by the product $\rho\, U_{eff}$, with a weaker modulation by $C_f\; C_p\; P^{-2/3}$, as the latter term varies less strongly

than the former. The effective velocity is defined in the model as

$$U_{eff} = (U_x^2 + U_y^2 + 2k)^{1/2} \quad (6)$$

where U_x and U_y are the two "outer flow" velocity components parallel to the surface in question outside of the boundary layer, and k is the kinetic energy of turbulence. This means that the model has to have the means of calculating all three mean velocity components and k. Further, equation (5) requires the knowledge of the skin friction coefficient C_f, which is modeled according to standard boundary layer theory and correlated with data obtained in flat plate boundary layers and fully developed pipe flow, i.e.,

$$C_f = a\,(\rho\, U_{eff}\, \delta/\mu)^{-1/4} \quad (7)$$

where the constant a has a value of 0.046 in flat plate boundary layers and 0.067 for fully developed pipe flow. At present, we use the mean of these two values.

The model calculates velocities and turbulence adjoining each of a number of forty resolved individual in-cylinder surfaces and from these it determines the local heat transfer coefficients through the Colburn analogy. To calculate the flow velocities, the flow model divides the combustion chamber volume into four regions. Two of the regions are inside the piston and head depressions (if any), respectively, one region is in the outside region above the piston, and the last one is the central core that remains.

The approach adopted treats each region in much the same way one handles an individual grid element in a detailed Navier-Stokes discretization. This means that only the mean motions on the scale of the element are resolved. The smaller scale motions which cannot be resolved are lumped into turbulence. Thus, the turbulence kinetic energy discussed here includes a wide range of scales, from the microscales up to the relatively chaotic smaller scale mean motions. This turbulence evolves under the influence of the external resolved mean velocity and strain field.

In each of the four flow regions one has to solve for the following quantities: radial velocity, axial velocity, swirl, turbulence intensity, and turbulence length scale. The models used are briefly described below, with more details available in Morel and Keribar (8).

Radial and Axial Velocities

The first two velocity components, axial and radial, are calculated, when possible, from mass conservation and from piston kinematics. For the axial velocity component this means the piston motion relative to the cylinder wall, and for the radial component it is the squish and reverse squish velocity along the piston crown where the flow is one-dimensional and the approximation is appropriate. Other radial and axial velocity components such as inflow into a cup or valve flow are essentially three-dimensional, and cannot be obtained without a detailed solution of Navier-Stokes equations. Those elements of the flow field are lumped into turbulence.

Swirl Equation

The swirl component is obtained from the solution of a differential equation for angular momentum in each of the four flow regions. The assumption is made that, in each region separately, the flow spins with a constant angular velocity (solid body rotation). The governing equation for each region is

$$(I_j\omega_j)^{\cdot} = \Sigma \dot{m}_{ij}\omega_{ij}r_{ij}^2 + \Sigma\rho U_{dif}\,(\omega_i-\omega_j)\int r^2 dA + \dot{m}_{int}M_{int} - \dot{m}_{exh}\omega_j r_j^2 + 1/2\rho\int C_f r^3 \omega_j dA$$

where subscript j refers to the region at hand, subscript i refers to the adjoining regions, subscript ij refers to situations where the subscript is either i or j depending on the flow direction across the region boundary and U_{dif} is a diffusion velocity proportional to the square root of turbulence energy. The swirl model includes the effects of squish which forces gas from region 1 into region 2, where the swirl is amplified. The swirl is set up during the induction period after which the angular momentum is gradually dissipated by the action of viscous friction on the surrounding walls.

Turbulence Equations

As already described above, turbulent kinetic energy is defined in broader terms to account for the insufficient spatial resolution. Its evolution is modeled by the widely used k-ϵ turbulence model. Integrating the equations over each of the

flow regions, one obtains a set of eight coupled ordinary differential equations which have to be integrated simultaneously in time. Both k and ϵ are assumed to be uniform over each flow region. The governing equations include the following terms:

1. generation of turbulence;
2. viscous decay by turbulent dissipation rate;
3. convection from zone to zone;
4. length scale limitation by action of boundary layers.

The equations are written in a form similar to the swirl equation

$$(m_j k_j)^{\cdot} = \Sigma \dot{m}_{ij} k_{ij} + \Sigma \rho U_{diff} (k_i - k_j) A + m_j S_k + \dot{m}_{int} k_{int} - \dot{m}_{exh} k_j + \dot{m}_{inj} k_{inj} + \dot{m}_{sq} k_{sq} \quad (8)$$

$$(m_j \epsilon_j)^{\cdot} = \Sigma \dot{m}_{ij} \epsilon_{ij} + \Sigma \rho U_{diff} (\epsilon_i - \epsilon_j) A + m_j S_\epsilon + \dot{m}_{int} \epsilon_{int} - \dot{m}_{exh} \epsilon_j + \dot{m}_{inj} \epsilon_{inj} + \dot{m}_{sq} \epsilon_{sq} + k_j^2 / L_j^2 \quad (9)$$

The details pertaining to these equations are given in Morel and Keribar (7).

When one averages the heat transfer coefficients over all of the surfaces, one can compare the resulting curve for example to the Annand and Woschni correlations, which are meant to be applied uniformly to all surfaces. This has been done for illustration purposes in Figure 1. It is seen that the flow-based model exhibits sensitivity to the in-cylinder flow development: it produces high values of heat transfer coefficients during the suction period due to the highly turbulent inlet flows; it calculates high heat transfer coefficients near TDC due to squish and compression generated turbulence; finally it calculates low heat transfer coefficients during the relatively quiescent expansion and discharge periods. An exception is the peak recurring right after TDC, which is produced by backflows into the cylinder through the discharge valve. By contrast, the Annand and Woschni correlations show none of these flow-related features.

EXPERIMENTAL VALIDATION

The convective heat transfer model has been originally developed for internal combustion engine applications, and has since been extensively tested against experimental data obtained in diesel and spark ignited engines (9, 10). Comparisons made for both non-fired and firing conditions showed an excellent agreement of the present model with detailed time-resolved heat flux measurements. No comparisons have yet been available for applications to reciprocating compressors, but considering the basic similarity of compressors to motoring engines one expects that the agreement with experiments will extend to that application.

HEAT CONDUCTION IN COMPRESSOR STRUCTURE

To calculate mean heat transfer between the compressing gases and the walls requires the knowledge of wall temperatures. Wall temperatures have to be either 1) known from previous measurements obtained at the same operating conditions, and specified as input; or 2) calculated using a heat conduction model. IRIS-C accommodates both approaches, although the second one is clearly the preferred approach in prediction calculations. It is the one that is normally used.

The structural heat conduction model establishes a complete, two-way coupling between the simulation of gas heat transfer and the heat conduction in the structure. On the gas side, the convection heat transfer model computes the distribution of heat fluxes along the walls, which provide boundary conditions for heat conduction calculations. The conduction calculations solve for the temperature distribution in the structure, including wall temperatures needed as boundary conditions in the cycle simulation. This coupling is automatic. As the cycle simulation iteration converges, the simultaneous conduction calculations drive towards a balance of the gas-to-structure and structure-to-coolant heat transfer. Several shaft revolutions (4-6) are needed to attain a thermal balance, and at that point consistent results for performance and component temperatures are obtained.

The structural heat conduction solver is a general finite element solver. It computes steady-state profiles or, during compressor transients, the structure's thermal response to speed/load changes. In the context of a distributed computational model (e.g. finite differences or FEM) the heat conduction equation is expressed as:

$$[C]\,\dot{T} + [K]\,T = \text{thermal load vector} \quad (10)$$

where [C] and [K] are heat capacitance and conductance matrices respectively, and T is the nodal temperature vector. Convective and frictional heat deposition/

extraction rates at individual boundary nodes constitute the thermal load vector applied in a spatially resolved manner. 1-D, 2-D or 3-D FEM models are allowed, with boundary faces represented by point, line or area elements. The FEM models can be quite simple scalar elements, which for heat conduction are the thermal resistances between any two nodal points. Using such elements, quasi-dimensional thermal resistance network representations of compressor structures can be constructed, which are analogous to electrical resistance networks. An IRIS-C pre-processor generates such networks using geometry and material property input data. Alternatively, one can use full finite element models of part or all of the compressor structure interfacing with any FEM code (e.g. ANSYS or NASTRAN).

During the design process, it is often desirable to compute detailed temperature profiles in part of the structure or a single component (e.g. piston cylinder). Other parts of the compressor structure are important only insofar as they describe heat paths to and from the area of interest. The procedure described above is especially suited to this purpose. For example, when a piston thermal finite element analysis is to be carried out, a detailed FEM model of the piston can be used together with a simple network representation for the rest of the structure.

Examples of different approaches to conduction modeling are shown in Figure 2. When performance is the main objective, determination of main heat paths is needed, one can use coarser, yet well resolved, representation of the structure as shown in Figure 2a, which contains 159 elements. When details of temperature distribution or thermal stresses are the objective, one can use a finite element model of arbitrary resolution, as shown in Figure 2b for a diesel engine piston. It should be noted that even with addition of FEM representation the computational expense is quite acceptable. With a simple coarse structural model the code executes in less than one minute CPU time on VAX 11/780, and a more detailed FEM model may increase this to several minutes.

APPLICATION TO A SMALL AIR COMPRESSOR

An analysis was made of a small three-cylinder single-acting air compressor with 75 mm bore and 56 mm stroke at nominal operating conditions defined by 1750 rpm, suction pressure of 1 bar, suction temperature of 308 K, discharge pressure of 5 bars and clearance volume 4 percent of the displacement volume, which is the same as that considered in (1).

Baseline Operating Point

At the baseline (nominal) operating point the compressor delivered 59.5 kg/hr of air with volumetric efficiency of 68 percent. The isothermal efficiency (defined in (1)) was 25.7%. The heat transfer rate was 8.8 percent of the input shaft work.

The details of the heat transfer process at this operating condition are quite interesting. In Figure 3 one can see the in-cylinder heat transfer rate as a function of crankangle. Not surprisingly, the heat transfer increases during the compression and peaks at the time of maximum pressure (discharge valve opening). Past that point it decreases due to fluid motion and turbulence decay (Figure 4) and due to reduced in-cylinder surface area as piston ascends. After TDC there is a secondary peak. This peak is produced by backflows into the cylinder which stir up the in-cylinder air and increase the heat transfer coefficient. Corresponding peaks can be seen in Figure 4 and in Figure 1. Finally, during the suction period, there is a large generation of turbulence in the cylinder which increases the heat transfer coefficient and produces the negative lobe in Figure 3, pertaining to heat transfer from the cylinder walls to the freshly inducted air. This reverse heat transfer has negative effect on volumetric efficiency as will be seen later.

Since the conduction solution tracks heat fluxes in the structure all the way to the coolant, its output provides a picture of all heat paths from the compressing gases to the coolant. One can for example draw the global heat paths as done in Figure 5. It can be seen that the rate of heat deposited from the gas on the compressor surfaces is 111 W for the piston, 83 W for the head and 72 W for the cylinder. In addition 136 W is deposited as friction-generated heat at the piston-cylinder interface. The heat flows through the piston in two directions: to the cylinder and to the piston underside cooled by air and crankcase oil. It also flows through the cylinder wall to the coolant and from the bottom of the cylinder to the crankcase oil.

Parametric Studies

These parametric studies were run to study the effect of operating parameters

on heat transfer and of heat transfer on compressor performance. Two of these, effect of pressure ratio and rpm, were the same as those discussed in reference (1). Decreasing pressure ratio was found to increase heat transfer monotonically, from about 5% of input work to anywhere between 9 and 16 percent depending on the clearance volume (Figure 6). Increasing the clearance volume further increases the heat transfer fraction. It may be noted in Figure 6 and in later figures that the heat transfer curves are not always smooth. This is the result of changes in the operating conditions on the discharge valve dynamics. Thus, the backflow producing the heat transfer increase at TDC in Figure 3 changes in magnitude and produces different levels of in-cylinder heat transfer. As for the effect of compressor speed, the heat transfer as a fraction of the input power decreases slightly with increasing compressor speed (Figure 7).

The reverse question may be posed, i.e. what is the effect of heat transfer on performance. In this context one can consider the following effects: the effect of level of compressor cooling, increase of heat transfer by promoting in-cylinder motions and effect of compressor size. All of these three aspects have been investigated. The effect of cooling was addressed by changing the coolant temperature. It was found that the coolant temperature affected significantly the heat transfer level, which decreased by almost a factor of two over the 40 K range of the study (Figure 8). This produced a slight concurrent drop in volumetric efficiency by two percentage points from 74% down to 72%. The discharge temperature rose by about one half the increase in the coolant temperature and the average in-cylinder wall temperature rose by about 33 K. The isothermal efficiency dropped from 22.8% to 22.1%, indicating that enhanced cooling improves isothermal efficiency (Figure 9).

Another study considered the effect of varying the in-cylinder heat transfer coefficient. Here again it was found that increasing the heat transfer, this time by enhancing the in-cylinder heat transfer coefficient, increased the isothermal efficiency. A limiting case considered was one where the heat transfer coefficient was made 300 times larger. This kept the air temperature at all times close to the suction temperature 308 K, approximating a true isothermal compression. The result was an increase in heat transfer to 80 per cent of input power and a significant increase in isentropic efficiency to 27%.

A final study was that of compressor size, extending from a bore diameter of 25 mm to 225 mm keeping bore/stroke ratio fixed. The mean piston speed was maintained at 3.3 m/sec by varying the compressor rpm inversely with bore and stroke. As expected, because of the changes in the surface area/volume ratio, the heat transfer fraction decreased with increasing compressor size from almost 11 percent down to 6.6 percent (Figure 10). The isothermal efficiency was also found to be dependent on the compressor size, increasing gradually with bore diameter (Figure 11).

CONCLUSIONS

1. New methodology has been developed to predict heat transfer in reciprocating compressors. It uses predictions of in-cylinder velocities to calculate heat transfer coefficients as a function of speed, pressure ratio, fluid properties and compressor valve and piston geometry. It has sensitivity to design detail, accounting for example for the effects of valve backflows which can affect the overall heat transfer level.

2. The temperature distribution in the compressor structure and the cooling load are calculated simultaneously with the compressor performance by coupling full structural heat transfer description with the thermodynamic model.

3. Parametric studies have been carried out to quantify the effects of compressor speed, pressure ratio, clearance volume and compressor size on heat transfer. The effect of coolant temperature on heat transfer and efficiency has also been addressed and quantified.

REFERENCES

1. Morel, T. and Keribar, R. (1988), "Comprehensive Model of A Reciprocating Compressor Applicable to Component Design Issues", Purdue Compressor Conference, 1988.

2. Nusselt, W. (1923), "Der Waermeuebergang in der Verbrennungskraft- maschine", Z. Ver. Dtsch. Ing., Vol. 67, p. 692.

3. Eichelberg, G. (1939), "Some New Investigations on Old Combustion-Engine Problems", Engineering, Vol. 148, p. 547.

4. Annand, W. D. (1963), "Heat Transfer in the Cylinders of Reciprocating Internal Combustion Engines", Proc. Instn. Mech. Engnrs., Vol. 177, No. 36, p. 973.

5. Woschni, G. (1967), "A Universally Applicable Equation for the Instantaneous Heat Transfer Coefficient in the Internal Combustion Engine", SAE Transactions, Vol. 76, p. 3065.

6. Borgnakke, C., Arpaci, V. S. and Tabaczynski, R. J. (1980), "A Model for Instantaneous Heat Transfer and Turbulence in a Spark Ignition Engine", SAE Paper 800287.

7. Davis, G. C. and Borgnakke, C. (1982), "The Effect of In-Cylinder Flow Processes (Swirl, Squish and Turbulence) on Engine Efficiency - Model Predictions", SAE Paper 820045.

8. Morel, T. and Keribar, R. (1985), "A Model for Predicting Spatially and Time Resolved Convective Heat Transfer in Bowl-in-Piston Combustion Chambers", SAE Paper 850204.

9. Morel, T., Wahiduzzaman, S., Tree, D. L. and DeWitt, D. P. (1987), "Effect of Speed Load and Location on Heat Transfer in a Diesel Engine--Measurements and Predictions", SAE Paper 870154.

10. Morel, T., Rackmil, C. I., Keribar, R. and Jennings, M. J. (1988A), "Model for Heat Transfer and Combustion in Spark Ignited Engines and Its Comparison with Experiments", SAE Paper 880198.

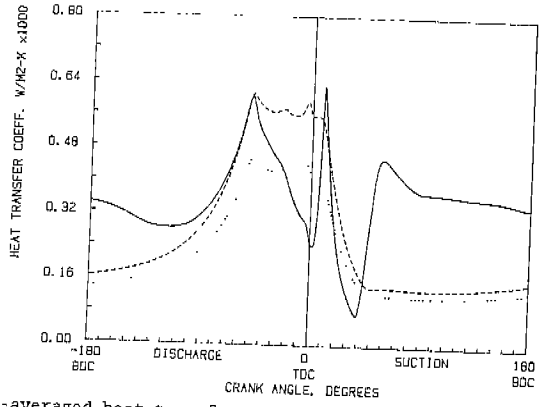

Figure 1. Area-averaged heat transfer coefficient calculated by the flow model and its comparison to two heat transfer correlations. ——— flow model, - - - Annand, ... Woschni.

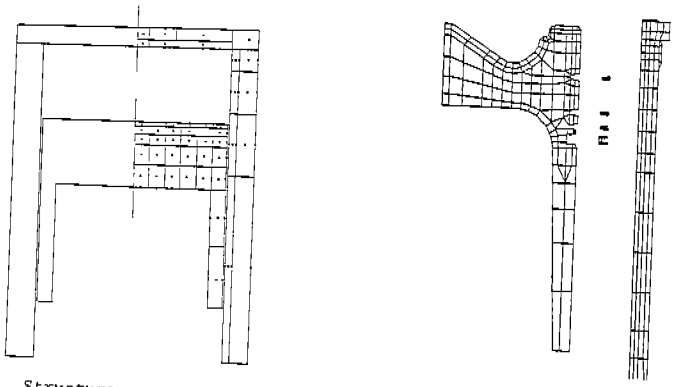

Figure 2. Structure representation for heat conduction calculations. a) medium resolution used for performance calculations, b) high resolution used for component temperature predictions and cooling calculations.

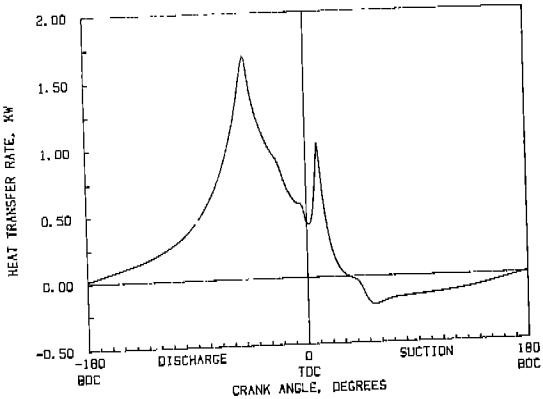

Figure 3. In-cylinder heat transfer rate as a function of crank angle.

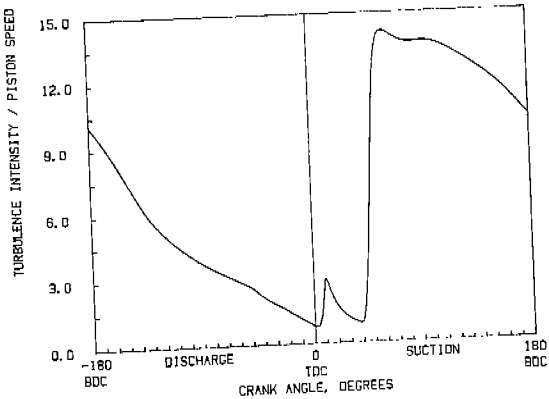

Figure 4. Turbulence intensity as a function of crank angle.

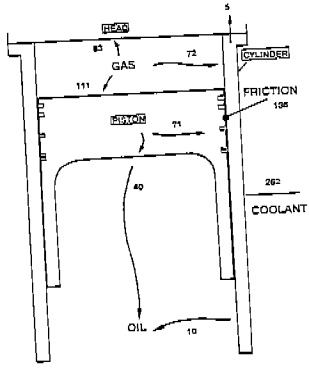

Figure 5. Heat paths in the compressor assembly at the baseline operating point. All fluxes are expressed in W.

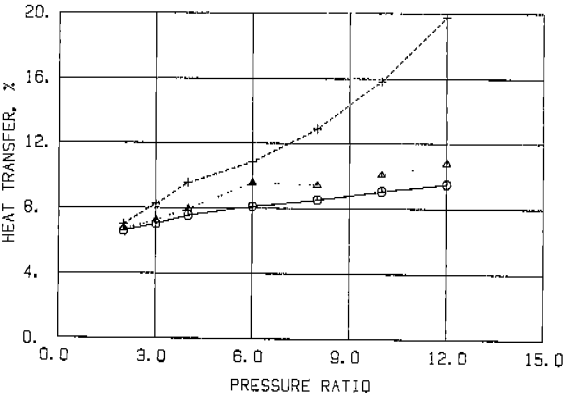

Figure 6. Effect of discharge pressure and clearance volume on the ratio of heat transfer to compressor input power. Clearance volume: ——— 2%, ... 4%, - - - 10%.

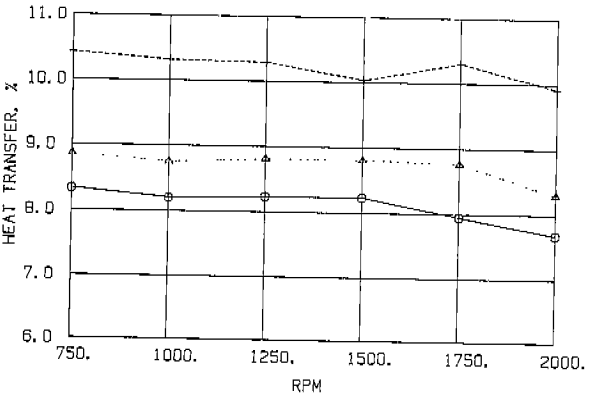

Figure 7. Effect of compressor speed and clearance volume on the ratio of heat transfer to compressor input power. Clearance volume: ——— 2%, ... 4%, - - - 10%.

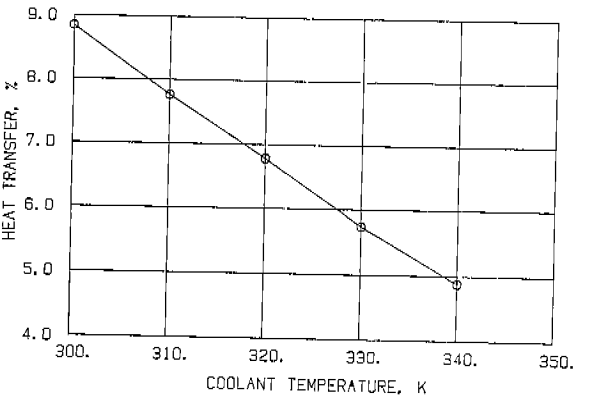

Figure 8. Effect of coolant temperature on the ratio of heat transfer to compressor input power.

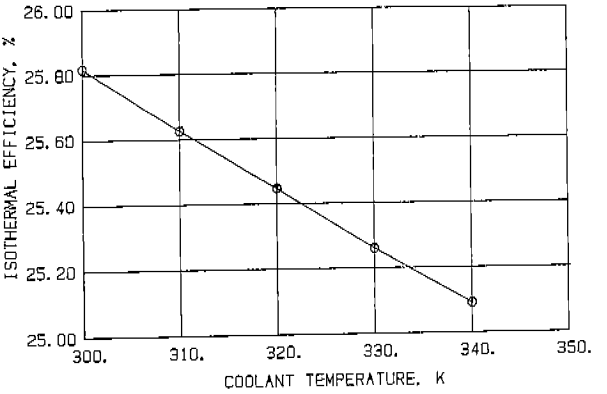

Figure 9. Effect of coolant temperature on isothermal efficiency.

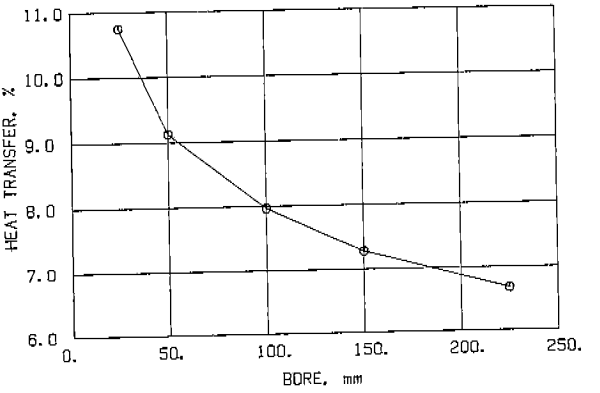

Figure 10. Effect of compressor size on the ratio of heat transfer to compressor input power.

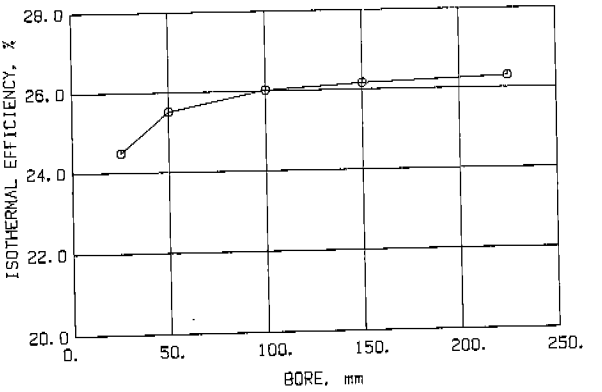

Figure 11. Effect of compressor size on isothermal efficiency.